Uncoupling Sae2 Functions in Downregulation of Tel1 and Rad53 Signaling Activities

Chiara Vittoria Colombo, Luca Menin, Riccardo Ranieri, Diego Bonetti, Michela Clerici,[1] and Maria Pia Longhese[1]

Dipartimento di Biotecnologie e Bioscienze, Università degli Studi di Milano–Bicocca, 20126 Milan, Italy

ORCID ID: 0000-0003-1726-2034 (M.P.L.)

ABSTRACT The Mre11-Rad50-Xrs2 (MRX) complex acts together with the Sae2 protein to initiate resection of DNA double-strand breaks (DSBs) and to regulate a checkpoint response that couples cell cycle progression with DSB repair. Sae2 supports resistance to DNA damage and downregulates the signaling activities of MRX, Tel1, and Rad53 checkpoint proteins at the sites of damage. How these functions are connected to each other is not known. Here, we describe the separation-of-function *sae2-ms* mutant that, similar to *SAE2* deletion, upregulates MRX and Tel1 signaling activities at DSBs by reducing Mre11 endonuclease activity. However, unlike *SAE2* deletion, Sae2-ms causes neither DNA damage sensitivity nor enhanced Rad53 activation, indicating that DNA damage resistance depends mainly on Sae2-mediated Rad53 inhibition. The lack of Sae2, but not the presence of Sae2-ms, impairs long-range resection and increases both Rad9 accumulation at DSBs and Rad53–Rad9 interaction independently of Mre11 nuclease activity. Altogether, these data lead to a model whereby Sae2 plays distinct functions in limiting MRX-Tel1 and Rad9 abundance at DSBs, with the control on Rad9 association playing the major role in supporting DNA damage resistance and in regulating long-range resection and checkpoint activation.

KEYWORDS MRX; Rad9; Rad53; Sae2; Tel1

MECHANISMS devoted to repair DNA lesions are essential for maintaining genome integrity. Among DNA lesions, DNA double-strand breaks (DSBs) are the most severe because they have the potential to cause loss of genetic information and chromosomal rearrangements (Mehta and Haber 2014). DSBs can be repaired by homologous recombination (HR), which requires that the 5′ strands of both DSB DNA ends are nucleolytically degraded (resected) (Bonetti *et al.* 2018). Then, the resulting 3′-ended single-stranded DNA (ssDNA) tails can invade an undamaged homologous DNA template, like the sister chromatid or the homologous chromosome (Mehta and Haber 2014).

In both yeast and mammals, DNA end resection is a two-step process. First, the Sae2 protein (CtIP in mammals) activates a latent endonuclease activity of Mre11 within the context of the Mre11-Rad50-Xrs2 (MRX) complex to incise the 5′-terminated strands at both DNA ends (Cannavo and Cejka 2014). The resulting nick generates an entry site for the Mre11 exonuclease, which degrades back toward the DSB end in the 3′–5′ direction, and for the long-range resection nucleases Exo1 and Dna2 that degrade away from the DSB in the 5′–3′ direction (Mimitou and Symington 2008; Zhu *et al.* 2008; Cejka *et al.* 2010; Niu *et al.* 2010; Garcia *et al.* 2011; Nimonkar *et al.* 2011; Shibata *et al.* 2014; Reginato *et al.* 2017; Wang *et al.* 2017). In addition to a nucleolytic activity in the vicinity of the broken DNA ends, MRX has a structural role in recruiting and promoting the activity of Exo1 and Dna2 at DNA DSBs (Cejka *et al.* 2010; Nicolette *et al.* 2010; Niu *et al.* 2010; Shim *et al.* 2010; Cannavo *et al.* 2013; Gobbini *et al.* 2018).

The short-range resection catalyzed by MRX-Sae2 is particularly important for the processing of DNA ends that possess protein blocks at their 5′-terminated DNA strands, such as stalled topoisomerases or Spo11 in meiosis (Trujillo and Sung 2001; Neale *et al.* 2005; Cannavo and Cejka 2014). By contrast, it can be dispensable during the processing of

doi: https://doi.org/10.1534/genetics.118.301830
Manuscript received October 16, 2018; accepted for publication December 9, 2018; published Early Online December 11, 2018.
Supplemental material available at Figshare: https://doi.org/10.25386/genetics.7392671.
[1]Corresponding authors: Università degli Studi di Milano–Bicocca, Piazza della Scienza 2, 20126 Milan, Italy. E-mail: mariapia.longhese@unimib.it; and michela.clerici@unimib.it

endonuclease-induced DNA breaks, whose DNA ends are readily accessible to Exo1 and Dna2 nucleases (Llorente and Symington 2004).

DSB generation triggers activation of the checkpoint protein kinases Mec1 and Tel1 (ATR and ATM in mammals, respectively), which sense and signal the presence of DNA DSBs, leading to arrest of cell cycle progression (Gobbini *et al.* 2013; Villa *et al.* 2016). The lack of any MRX/MRN subunit abolishes Tel1/ATM activation by preventing its association to DSBs (Nakada *et al.* 2003; Falck *et al.* 2005; Lee and Paull 2005; You *et al.* 2005; Berkovich *et al.* 2007), indicating that MRX/MRN is required for Tel1/ATM recruitment to DSBs. By contrast, Mec1/ATR (in association with Ddc2/ATRIP) recognizes the RPA-coated ssDNA that results from resection of the DSB DNA ends (Zou and Elledge 2003; Jazayeri *et al.* 2006; Myers and Cortez 2006). Once activated by damaged DNA, Tel1 and Mec1 propagate the checkpoint signals through the Rad53 and Chk1 effector kinases (Chk2 and Chk1 in mammals, respectively) (Ciccia and Elledge 2010). Rad53 activation requires the BRCT-domain-containing protein Rad9 (53BP1 in mammals). Rad9 undergoes Mec1- and/or Tel1-dependent phosphorylation upon DNA damage (Emili 1998; Vialard *et al.* 1998), and these phosphorylation events create a binding site for Rad53, thus allowing Rad53 in-trans autophosphorylation that leads to Rad53 activation as a kinase (Sun *et al.* 1998; Durocher *et al.* 1999; Pellicioli *et al.* 1999; Gilbert *et al.* 2001; Schwartz *et al.* 2002; Sweeney *et al.* 2005; Smolka *et al.* 2007).

Cells lacking *SAE2* are more sensitive to DNA damaging agents than *mre11* nuclease-dead mutants (Bonetti *et al.* 2015), indicating that Sae2 has Mre11-nuclease independent roles in the DNA damage response. Consistent with this hypothesis, the lack of Sae2 enhances Tel1 signaling activity by increasing MRX and Tel1 persistence at the DSB ends (Usui *et al.* 2001; Lisby *et al.* 2004; Clerici *et al.* 2006, 2014). This persistent MRX-Tel1 activation in *sae2*Δ cells is associated with enhanced activity of the downstream checkpoint kinase Rad53, which causes a permanent cell cycle arrest (Usui *et al.* 2001; Clerici *et al.* 2006). The increased MRX-Tel1-Rad53-mediated checkpoint activation has been proposed to account for the DNA damage hypersensitivity and the resection defect of *sae2*Δ cells. In fact, *mre11* mutant alleles that reduce MRX binding to DSBs restore DNA damage resistance and resection in *sae2*Δ cells (Chen *et al.* 2015; Puddu *et al.* 2015; Cassani *et al.* 2018). A similar effect also occurs when Tel1 function is affected by reducing either its association to DSBs or its kinase activity (Gobbini *et al.* 2015). Moreover, impairment of Rad53 activity by affecting either its interaction with Rad9 or its kinase activity suppresses both the hypersensitivity to DNA damage and the resection defect of *sae2*Δ cells (Gobbini *et al.* 2015).

Tel1 and Rad53 hyperactivation in *sae2*Δ cells leads to an increased accumulation of Rad9 at DSBs, which acts as a barrier to Sgs1-Dna2-mediated DSB resection (Bonetti *et al.* 2015; Ferrari *et al.* 2015; Gobbini *et al.* 2015). Furthermore, as Rad53 is known to phosphorylate and inhibit Exo1 (Morin *et al.* 2008), Rad9-mediated Rad53 hyperactivation in *sae2*Δ cells also leads to Exo1 inhibition. These findings lead to a model whereby the DNA damage hypersensitivity and the resection defect of *sae2*Δ cells are due to an increased MRX-Tel1 activation, which, in turn, leads to an increased Rad9 association at DSBs and Rad53 hyperactivation, thereby inhibiting Exo1 and Dna2-Sgs1 resection activity (Bonetti *et al.* 2018).

To better understand the contribution of MRX, Tel1, and Rad53 to the DNA damage hypersensitivity of Sae2-lacking cells, and how Sae2 modulates the signaling activities of the above factors, we searched for *sae2* alleles that failed to inhibit Tel1 but retained Sae2 function in supporting DNA damage resistance. Here, we describe the hypomorphic *sae2-ms* allele that, similar to *sae2*Δ and *mre11* nuclease defective alleles, increases MRX and Tel1 persistence at DSBs by affecting MRX cleavage activity. However, unlike *SAE2* deletion, the Sae2-ms mutant variant is capable of supporting DNA damage resistance and long-range resection, indicating that the enhanced MRX persistence at DSBs is not responsible for the increased DNA damage sensitivity and the resection defect of *sae2*Δ cells. Furthermore, unlike *SAE2* deletion, Sae2-ms does not enhance Rad53 activation, indicating separable functions of Sae2 in the downregulation of MRX-Tel1 and Rad53 signaling activities. Accordingly, the lack of Sae2, but not the presence of Sae2-ms, increases Rad9 association at DSBs and Rad53-Rad9 interaction independently of MRX nuclease activity. Altogether, these data indicate that Sae2 limits MRX association at DSBs and therefore Tel1 activation in a nuclease-dependent manner. Furthermore, it limits Rad9 persistence at DSBs and this inhibition plays the major role in supporting DNA damage resistance and in regulating both long-range resection and checkpoint activation.

Materials and Methods

Yeast strains

Strain genotypes are listed in Supplemental Material, Table S1. Strain YJK40.6, used to detect end-tethering, was kindly provided by D. P. Toczyski (University of California, San Francisco). Strain HS21, used to detect hairpin opening, was kindly provided by M. A. Resnick (National Institutes of Health, NC). Strains JKM139 and YMV45, used to detect DSB resection and single-strand annealing (SSA), respectively, were kindly provided by J. Haber (Brandeis University, Waltham). Cells were grown in YEP medium (1% yeast extract, 2% bactopeptone) supplemented with 2% glucose (YEPD), 2% raffinose (YEPR), or 2% raffinose and 3% galactose (YEPRG). Gene disruptions were generated by one-step PCR disruption method. All experiments were performed at 26°.

*Search for sae2 mutations that suppress mec1*Δ *sensitivity to HU and MMS*

To search for *sae2* alleles that suppress *mec1*Δ sensitivity to HU and MMS, but that do not impair Sae2 function in DSB

repair, we used low-fidelity PCR to random mutagenize the *SAE2* gene. Genomic DNA from a strain carrying the *LEU2* gene located 122 bp downstream of the *SAE2* stop codon was used as template to amplify by low-fidelity PCR a *SAE2* region spanning from position −54 to +212 bp from the *SAE2* coding sequence. Thirty independent PCR reaction mixtures were prepared, each containing 5 U GoTaq G2 Flexi DNA polymerase (Promega), 10 ng genomic DNA, 500 ng each primer, 0.5 mM each dNTP (dATP, dTTP, dCTP), 0.1 mM dGTP, 0.5 mM $MnCl_2$, 10 mM Tris-HCl (pH 8.3), 50 mM KCl and 3 mM $MgCl_2$. The resulting PCR amplification products, containing the *SAE2* coding sequence and the *LEU2* marker gene, were used to transform a *mec1*Δ *sml1*Δ mutant strain in order to replace the *SAE2* wild type sequence with the mutagenized DNA fragments. Transformant clones were selected on synthetic medium without leucine and then assayed by drop test for increased viability in the presence of HU and MMS compared to *mec1*Δ. Among them, the clones that, after transformation with a plasmid carrying the wild-type *MEC1* gene, showed camptothecin (CPT) and phleomycin (phleo) resistance compared to *sae2*Δ cells were chosen for further characterization.

DSB resection and repair by SSA

DSB end resection at the *MAT* locus in JKM139 derivative strains was analyzed on alkaline agarose gels by using a single-stranded probe that anneals to the unresected DSB strand on one side of the break (Colombo *et al.* 2018). Quantitative analysis of DSB resection was performed by calculating the ratio of band intensities for ssDNA to total amount of DSB products. DSB repair by SSA was detected by Southern blot analysis using an Asp718–Sal1 fragment containing part of the *LEU2* gene as a probe (Trovesi *et al.* 2011). Quantitative analysis of the repair product was performed by calculating the ratio of band intensities for SSA product with respect to a loading control.

Plasmid religation assay

The centromeric pRS316 plasmid digested with the *Bam*HI restriction enzyme was transformed into the cells. Efficiency of religation was calculated by determining the number of colonies that were able to grow on medium selective for the plasmid marker and was normalized respect to the transformation efficiency for each strain. Transformation efficiency was determined after transformation with undigested pRS316 DNA.

ChIP and qPCR

Chromatin immunoprecipitation (ChIP) analysis was performed with anti-HA (12CA5) and anti-Myc antibodies (Ab32 from Abcam) as previously described (Cassani *et al.* 2016). Quantification of immunoprecipitated DNA was achieved by quantitative real-time PCR (qPCR) on a Bio-Rad MiniOpticon apparatus. Triplicate samples in 20 μl reaction mixture containing 10 ng of template DNA, 300 nM of each primer, 2× SsoFast EvaGreen supermix (#1725201; Bio-Rad) (2× reaction buffer with dNTPs, Sso7d-fusion polymerase, $MgCl_2$, EvaGreen dye, and stabilizers) were run in white 48-well PCR plates Multiplate (#MLL4851; Bio-Rad). The qPCR program was as follows: step 1, 98° for 2 min; step 2, 98° for 5 sec; step 3, 60° for 10 sec; step 4, return to step 2 and repeat 30 times. At the end of the cycling program, a melting program (from 65 to 95° with a 0.5° increment every 5 sec) was run to test the specificity of each qPCR. Data are expressed as fold enrichment at the HO-induced DSB over that at the noncleaved *ARO1* locus, after normalization of each ChIP signal to the corresponding input for each time point. Fold enrichment was then normalized to the efficiency of DSB induction.

Western blotting and immunoprecipitation

Protein extracts for western blot analysis were prepared by trichloroacetic acid (TCA) precipitation and separated on 10% polyacrylamide gels. Rad53 was detected by using anti-Rad53 polyclonal antibodies kindly provided by J. Diffley (The Francis Crick Institute, London, UK), while Rad9 was detected by using anti-Rad9 polyclonal antibodies kindly provided by N. Lowndes (University of Ireland, Galway, Ireland). Epitope-tagged Mre11, Tel1, Rad9, and Sae2 were detected by using anti-HA (12CA5) or anti-Myc antibodies (Ab32 from Abcam). Rad53–Rad9 coimmunoprecipitations were performed as previously described (Schwartz *et al.* 2002). Sae2–Sae2 coimmunoprecipitations were performed as previously described (Kim *et al.* 2008).

Hairpin opening assay

The rate of Lys+ recombinants was derived from the median recombination frequency determined from 10 different isolates of each strain as previously described (Lobachev *et al.* 2002). Three trials were performed and the mean recombination rate was calculated.

Data availability

Table S1 includes names and genotypes of each strain used in this work. Figure S1 illustrates the DNA damage sensitivity of *sae2-ms* and *sae2-S134L* cells. All the strains are available upon request. All data necessary for confirming the conclusions of the article are present within the article and the associated supplemental files. Supplemental material available at Figshare: https://doi.org/10.25386/genetics.7392671.

Results

Search for sae2 alleles that hyperactivate Tel1 but do not cause DNA damage hypersensitivity

Cells lacking Sae2 are hypersensitive to DNA damaging agents and increase MRX occupancy at DSBs, which activates a Tel1-dependent checkpoint that is accompanied by persistent Rad53 phosphorylation and prolonged cell cycle arrest (Usui *et al.* 2001; Lisby *et al.* 2004; Clerici *et al.* 2006).

To gain insights into the role of Sae2 in DNA damage resistance and downregulation of the checkpoint response,

we searched for separation-of-function *sae2* mutants that hyperactivated Tel1, similar to *sae2*Δ cells, but conserved Sae2 function in DNA damage resistance. We took advantage of the finding that Tel1 hyperactivation allows *SAE2* deletion to suppress the hypersensitivity to hydroxyurea (HU) and methyl methanesulfonate (MMS) of cells lacking Mec1 and kept viable by *SML1* deletion (Usui *et al.* 2001). We randomly mutagenized the *SAE2* gene by low-fidelity PCR, followed by transformation of *mec1*Δ *sml1*Δ cells with the linear *SAE2* PCR products obtained, in order to replace the corresponding *SAE2* wild-type sequence with the mutagenized DNA fragments. Transformant clones were first chosen based on their increased viability in the presence of HU and MMS compared to *mec1*Δ cells. Among them, we selected for further characterization clones that were more resistant to camptothecin (CPT) and phleomycin (phleo) compared to *sae2*Δ cells after transformation with a plasmid carrying the wild-type *MEC1* gene.

By the above analysis we identified the *sae2-ms* allele, DNA sequencing of which revealed three missense mutations leading to replacement of Ser134 with Leu, Pro217 with Thr, and Ala230 with Val, respectively. Similar to *sae2*Δ *mec1*Δ cells, *sae2-ms mec1*Δ cells showed increased viability in the presence of HU or MMS compared to *mec1*Δ cells (Figure 1A), indicating that the *sae2-ms* allele compensates for Mec1 deficiency under genotoxic treatments. Unlike *SAE2* deletion, which, by itself, causes hypersensitivity to HU, MMS, CPT, and phleo, *sae2-ms* cells did not lose viability in the presence of any of the above tested drugs (Figure 1B), indicating that Sae2-ms maintains Sae2 function in DNA damage resistance.

*Sae2-ms supports viability of rad27*Δ *and sgs1*Δ *cells*

Synthetic lethality/sickness is observed when *SAE2* deletion is combined with deletion of the *RAD27* gene, which encodes a nuclease involved in Okazaki fragment processing during lagging strand DNA synthesis (Tishkoff *et al.* 1997), suggesting that Sae2 is required for the processing of DNA lesions generated in a *rad27*Δ background (Moreau *et al.* 1999; Debrauwère *et al.* 2001). A similar synthetic effect is also seen when *SAE2* is deleted in cells lacking the helicase Sgs1, possibly due to defective DSB resection and excessive telomere shortening (Mimitou and Symington 2008; Hardy *et al.* 2014).

To determine whether Sae2-ms maintains the Sae2 functions mentioned above, diploid cells heterozygous for both *rad27*Δ and *sae2-ms* or *sgs1*Δ and *sae2-ms* were generated, and, after sporulation, tetrads were dissected to determine whether viable *rad27*Δ *sae2-ms* or *sgs1*Δ *sae2-ms* spores could be obtained. As expected, *rad27*Δ *sae2*Δ and *sgs1*Δ *sae2*Δ spores were unviable or grew so slowly that they could not be further propagated (Figure 1C). By contrast, the *rad27*Δ *sae2-ms* and *sgs1*Δ *sae2-ms* spores grew remarkably well (Figure 1D). Furthermore, *sae2-ms* did not exacerbate the hypersensitivity to HU and CPT of *rad27*Δ (Figure 1E) and *sgs1*Δ cells (Figure 1F). These findings indicate that Sae2-ms maintains Sae2 function in supporting cell viability in the absence of Rad27 or Sgs1 both in the presence and in the absence of DNA damage.

Sae2-ms maintains Sae2 functions in end-tethering and long-range resection

Sae2 promotes DSB repair by supporting DNA-end resection and by maintaining the DSB ends adjacent to each other (Clerici *et al.* 2005). The lack of Sae2 affects not only short-range resection by abrogating Mre11 nuclease activity, but also reduces the efficiency of long-range resection by increasing the association of Rad9 at DSBs, which directly and indirectly inhibits the resection activity of Dna2-Sgs1 and Exo1, respectively (Morin *et al.* 2008; Bonetti *et al.* 2015; Ferrari *et al.* 2015; Gobbini *et al.* 2015).

The lack of Sae2 leads to severe defects in repairing a DSB by SSA (Clerici *et al.* 2005). This mechanism repairs a DSB flanked by direct DNA repeats when sufficient resection exposes the complementary DNA sequences, which can then anneal to each other, resulting in deletion of the DNA region between the repeats (Fishman-Lobell *et al.* 1992; Ivanov *et al.* 1996). To assess whether Sae2-ms affects DSB repair by SSA, we introduced the *sae2-ms* allele in the YMV45 strain, which carries two direct sequence repeats of the *LEU2* gene on chromosome III separated by 4.6 kb. An HO endonuclease cleavage site was inserted at the junction between one of the *leu2* repeats and the intervening sequence (Vaze *et al.* 2002) (Figure 2A). This strain also carries a *GAL-HO* construct that provides galactose-inducible *HO* expression. Accumulation of the SSA repair products after HO induction was reduced in *sae2*Δ cells compared to wild type, whereas it occurred with almost wild-type kinetics in *sae2-ms* cells (Figure 2, B and C), indicating that Sae2-ms does not affect DSB repair by SSA.

The SSA-mediated DSB repair defect in *sae2*Δ cells has been attributed to the lack of Sae2 function in both DNA-end tethering and long-range resection (Clerici *et al.* 2005). To assess more directly the ability of Sae2-ms to support end tethering, we used a strain where Lac repressor binding site (LacO) arrays were inserted at a distance of 50 kb on opposite sides of an irreparable HO-inducible cut site, and can be visualized by the binding of a constitutively expressed LacI-GFP fusion protein (Lobachev *et al.* 2002). HO expression was induced by galactose addition to cell cultures that were arrested and kept blocked in G2 by nocodazole treatment to ensure that all cells would remain arrested in metaphase. Most wild-type and *sae2-ms* cells showed a single LacI-GFP focus after HO induction, indicating their ability to maintain the broken DNA ends together, whereas *sae2*Δ cells showed an increase of cells with two LacI-GFP spots after HO induction (Figure 3A) (Clerici *et al.* 2005). Altogether, these findings indicate that Sae2-ms does not impair DNA end-tethering.

The lack of Sae2 was shown to reduce long-range resection of an endonuclease-induced DSB by increasing the amount of Rad9 bound DSBs, which, in turn, acts as a barrier to Sgs1-Dna2-mediated resection and inhibits Exo1 activity by

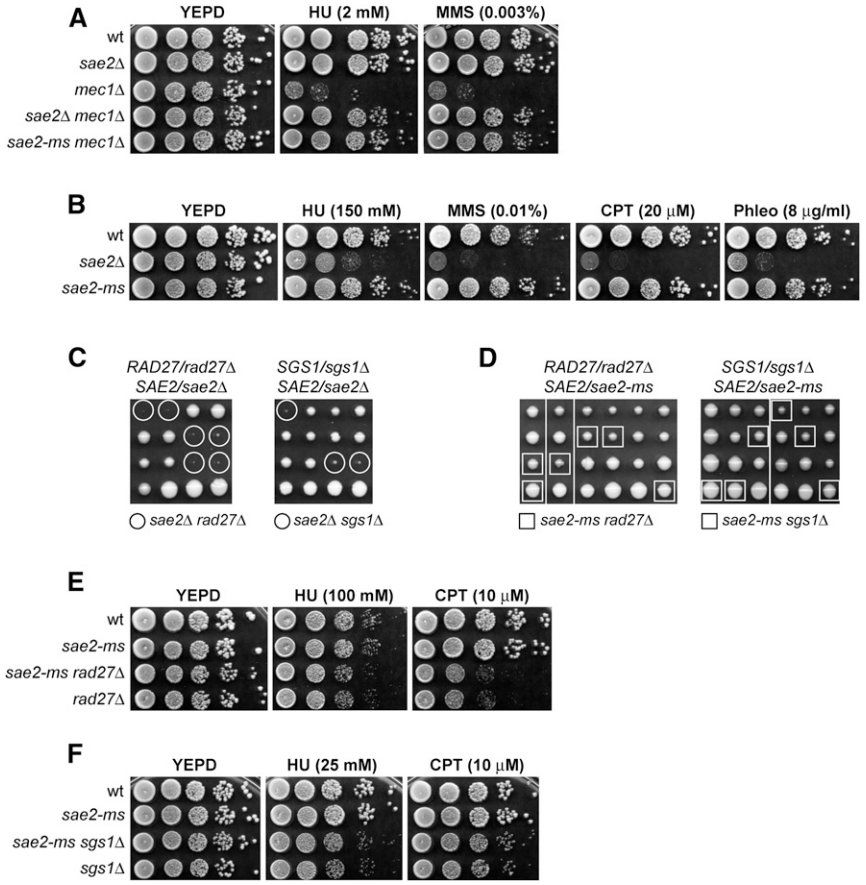

Figure 1 Sae2-ms suppresses the hypersensitivity to HU and MMS of *mec1*Δ cells. (A, B, E, and F) Exponentially growing cells were serially diluted (1:10) and each dilution was spotted out onto YEPD plates with or without HU, MMS, CPT, or phleo at the indicated concentrations. All strains in (A) carried *SML1* deletion that kept *mec1*Δ cells viable. (C and D) Meiotic tetrads were dissected on YEPD plates that were incubated at 25°, followed by spore genotyping.

activating Rad53 (Morin *et al.* 2008; Bonetti *et al.* 2015; Ferrari *et al.* 2015). To test more directly the ability of *sae2-ms* cells to support resection by Sgs1-Dna2 and Exo1, we monitored ssDNA formation and Rad9 persistence at the HO-induced DSB generated at the *MAT* locus in JKM139 derivative strains expressing the *HO* gene from the galactose-inducible *GAL1* promoter (Lee *et al.* 1998). The *HML* and *HMR* loci were deleted in these strains to prevent DSB repair by gene conversion. Resection of the HO-induced DSB renders the DNA sequence flanking the HO break resistant to cleavage by restriction enzymes, resulting in the appearance of resection intermediates that can be detected by Southern blot with a probe that anneals to the 3′ end at one side of the break (Figure 3B). As expected, *sae2*Δ cells showed a slight defect in resection of the HO-induced DSB compared to wild type, whereas the resection products accumulated with wild-type kinetics in *sae2-ms* cells (Figure 3, C and D). Furthermore, the amount of Rad9 bound at the HO-induced DSB, which was increased in *sae2*Δ cells compared to wild-type cells, was similar in both wild type and *sae2-ms* cells (Figure 3E). The increased Rad9 association at DSBs in *sae2*Δ cells is not due to altered Mre11 nuclease activity, as cells carrying the nuclease-dead *mre11-H125N* allele did not increase Rad9 persistence at the HO-induced DSB (Figure 3E).

Consistent with the ability of Sae2-ms to support long-range resection by Dna2 and Exo1, the *sae2-ms* mutation did not exacerbate the DNA damage hypersensitivity of *exo1*Δ cells, as it did *SAE2* deletion possibly because of a more severe resection defect of *sae2*Δ *exo1*Δ double mutant compared to each single mutant (Figure 3F) (Zhu *et al.* 2008). Furthermore, *sae2-ms* cells did not increase the efficiency of ligation by NHEJ of a self-replicating plasmid, which was instead increased in *sae2*Δ cells likely because the reduced ssDNA generation increases the ability of NHEJ repair events to occur (Figure 3G). Altogether, these findings indicate that Sae2-ms supports both DNA end-tethering and the activity of the long-range resection nucleases.

Suppression of Mec1 deficiency by Sae2-ms requires Tel1, Rad9, and Rad53

Tel1 promotes activation of the downstream effector kinase Rad53 in response to DNA damage, and this activation requires Rad9 (Gobbini *et al.* 2013). To assess whether suppression of the DNA damage hypersensitivity of *mec1*Δ cells by Sae2-ms is due to hyperactivation of a Tel1-mediated checkpoint response, we asked whether *mec1*Δ suppression by *sae2-ms* requires Tel1, Rad9, and/or Rad53. The *sae2-ms* allele failed to suppress the HU hypersensitivity of *tel1*Δ *mec1*Δ cells, which lose viability dramatically even in the absence of DNA damage compared to each single mutant (Figure 4A), possibly due to excessive telomere shortening and premature senescence (Ritchie *et al.* 1999). Similarly, *sae2-ms* did not restore HU resistance of *mec1*Δ cells carrying either *RAD9* deletion (Figure 4B) or the kinase defective

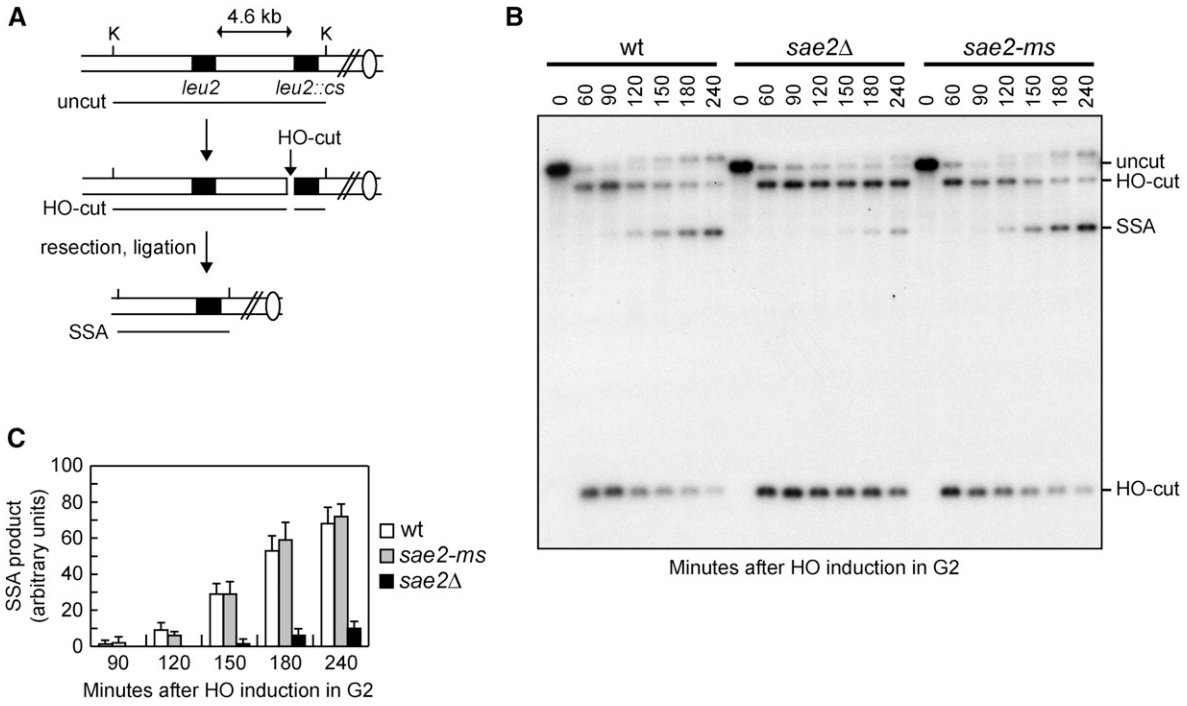

Figure 2 Sae2-ms is proficient in SSA-mediated DSB repair. (A) Map of the YMV45 chromosome III region where the HO-cut site is flanked by homologous *leu2* sequences that are 4.6 kb apart. HO-induced DSB formation results in generation of 12 and 2.5 kb DNA fragments (HO-cut) that can be detected by Southern blot analysis of *Kpn*I-digested genomic DNA with a *LEU2* probe. DSB repair by SSA generates a product of 8 kb (SSA). K, *Kpn*I. (B) Exponentially growing YEPR cell cultures were arrested in G2 with nocodazole and transferred to YEPRG in the presence of nocodazole at time zero to induce HO expression. Southern blot analysis of *Kpn*I-digested genomic DNA with a *LEU2* probe. (C) Densitometric analysis. The experiment as in (B) was repeated independently and the mean values are represented with error bars denoting SD (n = 3).

rad53-K227A allele (Figure 4C). These findings indicate that the bypass of Mec1 function by Sae2-ms requires Tel1, Rad9, and Rad53 checkpoint proteins. Consistent with a Tel1 involvement, suppression of the HU sensitivity of *mec1*Δ *sae2-ms* double mutant cells was unaffected by the lack of Ddc1 (Figure 4D), which interacts with Mec3 and Rad17 to form a heterotrimeric complex that stimulates Mec1 kinase activity but not Tel1 kinase activity (Gobbini *et al.* 2013).

The sae2-S134L mutation is responsible for suppression of Mec1 deficiency

The Sae2-ms mutant variant carries the three amino acid substitutions S134L, P217T, and A230V. We asked which substitution(s) was responsible for the suppression of *mec1*Δ hypersensitivity to DNA damage by constructing strains expressing the *sae2-S134L* or the *sae2-P217T*, *A230V* allele. Comparison analysis revealed that the *sae2-S134L* allele restored resistance of *mec1*Δ cells to HU and MMS to a level similar to that observed in *sae2-ms mec1*Δ cells, whereas the *sae2-P217T*, *A230V* allele did not (Figure 4E). Thus, effective *mec1*Δ suppression appears to be due exclusively to the S134L aminoacid substitution. Similar to *sae2-ms* cells, *sae2-S134L* cells were not hypersensitive to DNA damaging agents (Figure S1).

The Sae2 S134 residue was shown to be phosphorylated by Cdk1 (Huertas *et al.* 2008; Fu *et al.* 2014), prompting us to test the effect of substituting this residue with either the nonphosphorylatable alanine residue or aspartic acid, which mimics constitutive phosphorylation. We found that the *sae2-S134A* allele suppressed the HU and MMS sensitivity of *mec1*Δ cells as efficiently as *sae2-S134L* (Figure 4E). However, the S134D aminoacid substitution also restored resistance of *mec1*Δ cells to HU and MMS (Figure 4E), suggesting that the negative charge associated with the phosphorylation event of S134 is not relevant for Sae2 function in bypassing Mec1 deficiency. Consistent with this hypothesis, substitution of the E131 residue, which is located close to S134, with valine suppressed the sensitivity to MMS of *mec1*Δ cells without causing DNA damage hypersensitivity by itself (Kim *et al.* 2008), suggesting that the region of the protein surrounding the S134 residue, rather than its phosphorylation, is important for the bypass of Mec1 function.

Sae2-S134L and Sae2-ms reduce hairpin cleavage and increase MRX and Tel1 association at DNA DSBs

Previous work has established that *SAE2* deletion leads to increased MRX persistence at DSBs, which can account for enhanced Tel1 activation and bypass of Mec1 deficiency (Usui *et al.* 2001; Lisby *et al.* 2004; Clerici *et al.* 2006). Thus, we measured Mre11 and Tel1 association at the HO-induced DSB by ChIP and qPCR. Association to DNA DSBs of both Mre11 (Figure 5A) and Tel1 (Figure 5B) was more robust and persisted longer, not only in *sae2*Δ cells but also in *sae2-ms* and *sae2-S134L* cells, indicating that Sae2-ms and Sae2-S134L increase the amount of MRX and Tel1 bound at DSBs.

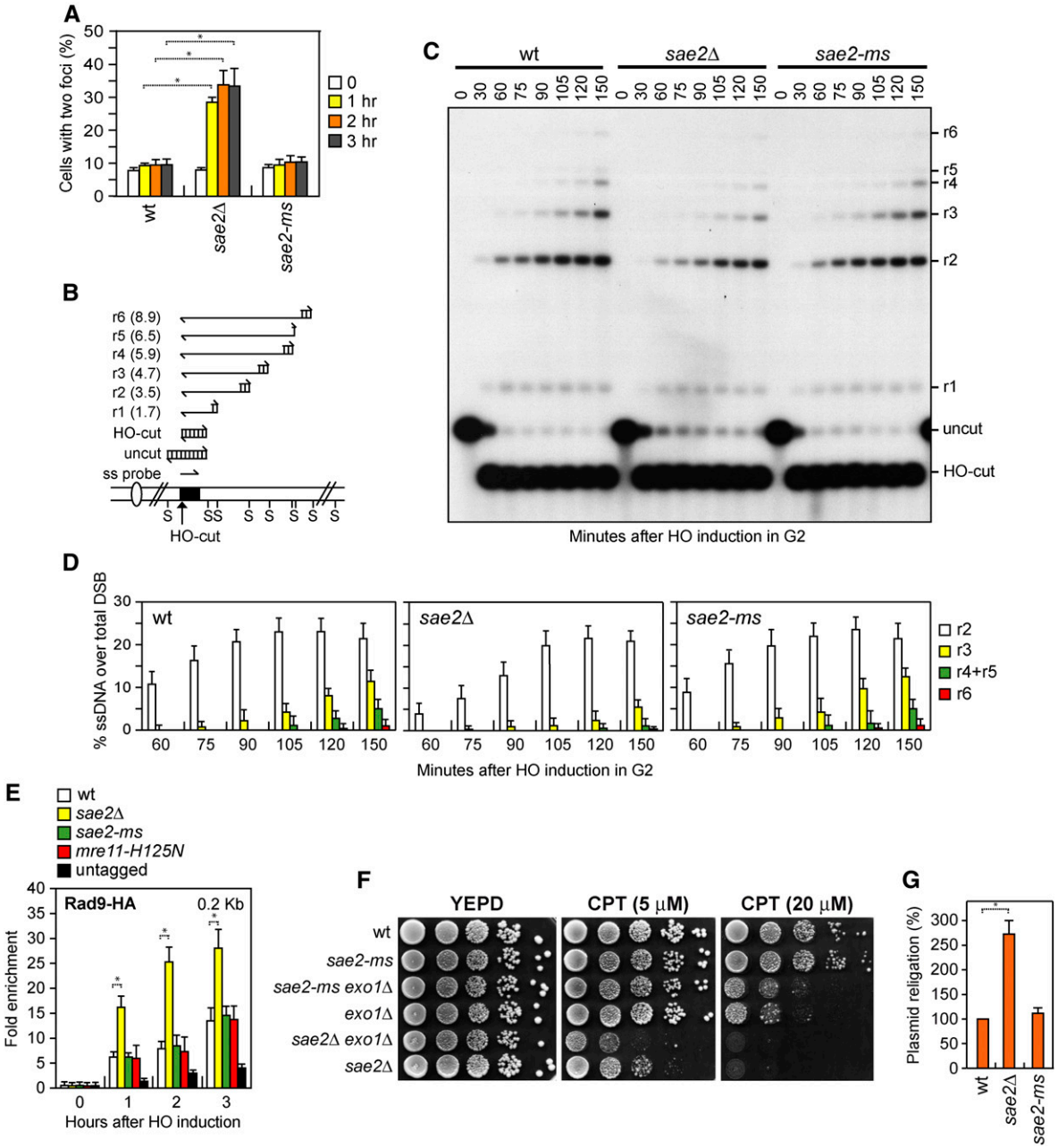

Figure 3 Sae2-ms is proficient in end-tethering and long-range resection. (A) DSB end-tethering. Exponentially growing YEPR cell cultures were arrested in G2 with nocodazole and transferred to YEPRG in the presence of nocodazole at time zero; 200 cells for each strain were analyzed to determine the percentage of cells showing two LacI-GFP foci. Plotted values are the mean values with error bars denoting SD ($n = 3$). * $P < 0.05$ (Student's *t*-test). (B) Map of the JKM139 chromosome III region. 5′–3′ resection progressively eliminates *Ssp*I sites, producing larger *Ssp*I fragments (r1 through r6). S, *Ssp*I. (C) DSB resection. YEPR exponentially growing cultures of JKM139 derivative strains were arrested in G2 with nocodazole and transferred to YEPRG in the presence of nocodazole at time zero to induce HO expression. *Ssp*I-digested genomic DNA was separated on alkaline agarose gel and hybridized with a single-stranded *MAT* probe that anneals to the unresected 3′ end at one side of the break. (D) Densitometric analysis. The experiment as in (C) was repeated independently and the mean values are represented with error bars denoting SD ($n = 3$). (E) ChIP analysis. HO was induced by galactose addition at time zero in exponentially growing JKM139 derivative cells. Relative fold enrichment of Rad9-HA protein at the indicated distance from the HO cleavage site was determined after ChIP with anti-HA antibodies and qPCR analysis. Plotted values are the mean values with error bars denoting SD ($n = 3$). * $P < 0.05$ (Student's *t*-test). (F) Exponentially growing cells were spotted out onto YEPD plates with or without CPT. (G) Plasmid religation assay. Data are expressed as percentage of religation relative to wild type that was set up at 100% after normalization to the corresponding transformation efficiency. Plotted values are the mean values with error bars denoting SD ($n = 3$). * $P < 0.05$ (Student's *t*-test).

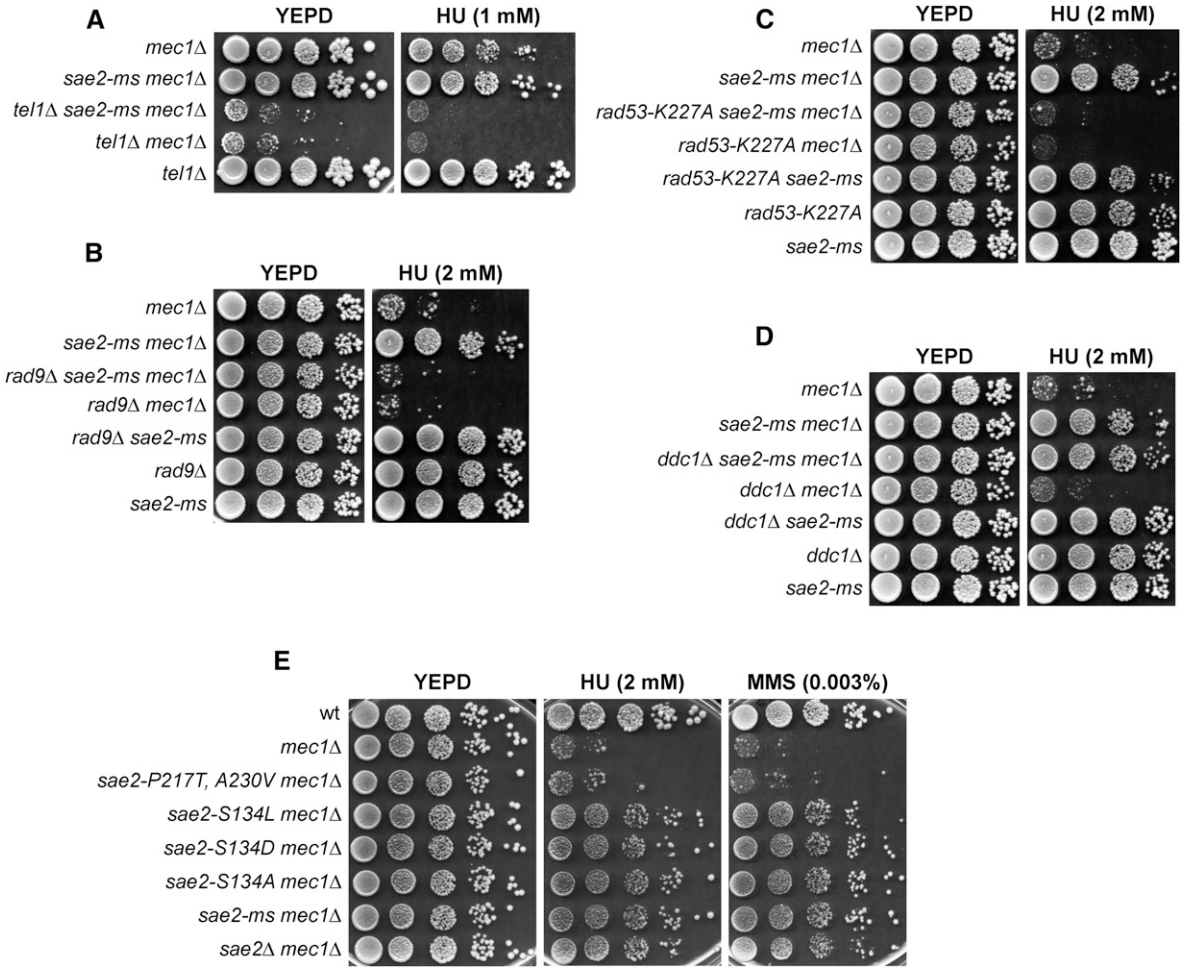

Figure 4 Sae2-ms requires Tel1, Rad53, and Rad9 for suppression of Mec1 deficiency. (A–E) Exponentially growing cells were serially diluted (1:10) and each dilution was spotted out onto YEPD plates with or without HU or MMS at the indicated concentrations. All strains carried *SML1* deletion that kept *mec1*Δ cells viable.

The increased Mre11 and Tel1 association was not due to increased amounts of Mre11 or Tel1, as similar levels of Mre11 (Figure 5C) and Tel1 (Figure 5D) proteins were detected in protein extracts from wild type, *sae2-ms*, and *sae2-S134L* cells.

The Sae2-dependent Mre11 endonucleolytic activity is essential to initiate resection at DNA ends that are not directly accessible to Exo1 and Dna2-Sgs1 because they are capped by hairpin DNA structures or bound proteins (Trujillo and Sung 2001; Lobachev *et al.* 2002; Cannavo and Cejka 2014). *mre11-H125N* allele, which specifically eliminates Mre11 nuclease activity, increases Mre11 and Tel1 persistence at DSBs (Figure 5, A and B) (Lisby *et al.* 2004; Clerici *et al.* 2006), suggesting that this activity can contribute to MRX displacement from DSBs. Thus, we investigated whether the *sae2-ms* and *sae2-S134L* mutations might specifically reduce Mre11 nuclease activity. As the Mre11 nuclease activity and Sae2 are required to open DNA hairpin structures both *in vitro* and *in vivo* (Trujillo and Sung 2001; Lobachev *et al.* 2002), we used a genetic assay to measure hairpin resolution in *sae2-ms* and *sae2-S134L* cells. Inverted Alu elements inserted in the *LYS2* gene on chromosome III form a hairpin-capped end, whose opening by the MRX nuclease and Sae2 stimulates recombination with a truncated *lys2* gene on chromosome II to generate Lys$^+$ cells (Lobachev *et al.* 2002). As expected, *sae2*Δ and the nuclease defective *mre11-H125N* cells showed decreased rates of Lys$^+$ recombinants compared to wild-type cells (Figure 5E). Interestingly, the rates of Lys$^+$ prototrophs were reduced also in *sae2-ms* and *sae2-S134L* cells, although to lower extents than in *sae2*Δ and *mre11-H125N* cells (Figure 5E). These findings suggest that Sae2-ms and Sae2-S134L can impair MRX removal from the sites of DNA damage by altering Mre11 nuclease activity.

Although Mre11-H125N persisted longer at DNA DSBs (Figure 5A) and caused increased Tel1 association at DSBs (Figure 5B), it did not suppress the hypersensitivity to HU of *mec1*Δ cells and only slightly suppressed their hypersensitivity to MMS (Figure 5F). This finding suggests that upregulation of MRX and Tel1 in the presence of the Mre11-H125N mutant variant is not sufficient to bypass Mec1 deficiency.

It has been shown that Sae2 oligomerization is important for Sae2 function in the DNA damage response (Kim *et al.*

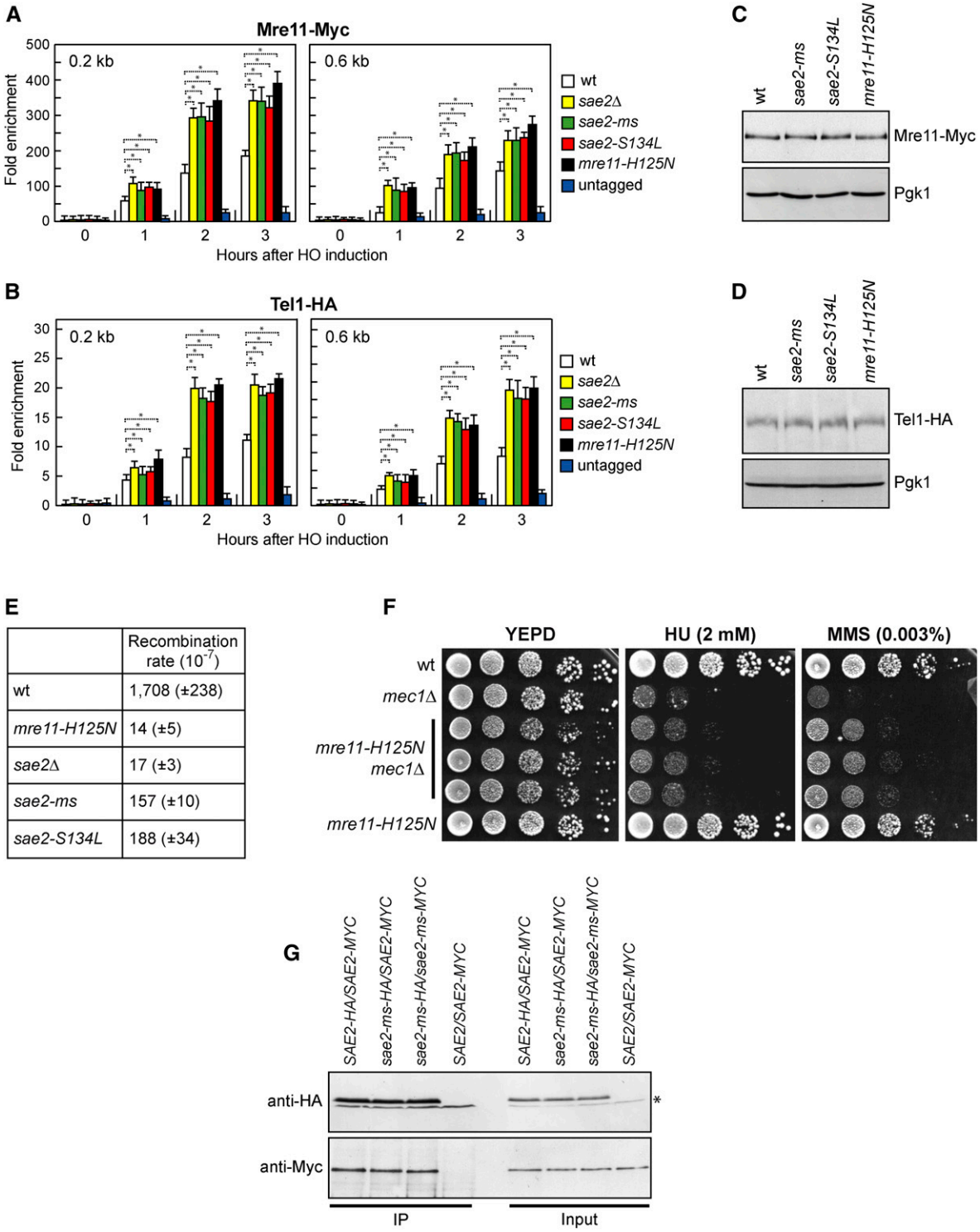

	Recombination rate (10^{-7})
wt	1,708 (±238)
mre11-H125N	14 (±5)
sae2Δ	17 (±3)
sae2-ms	157 (±10)
sae2-S134L	188 (±34)

Figure 5 Sae2-ms and Sae2-S134L enhance Mre11 and Tel1 association to DSBs and reduce hairpin cleavage. (A) ChIP analysis. HO was induced by galactose addition at time zero in exponentially growing JKM139 derivative cells. Relative fold enrichment of Mre11-Myc protein at the indicated distances from the HO cleavage site was determined after ChIP with anti-Myc antibodies and subsequent qPCR analysis. Plotted values are the mean values with error bars denoting SD ($n = 3$). * $P < 0.05$ (Student's *t*-test). (B) As in (A), but showing relative fold enrichment of Tel1-HA after ChIP with anti-HA antibodies. (C and D) Western blot analysis with anti-Myc or anti-HA antibodies of protein extracts prepared from exponentially growing cells. The same amount of extracts was probed with anti-Pgk1 antibodies as loading control. (E) Recombination frequency of strains with the *lys2-AluIR* and *lys2-Δ5′* ectopic recombination system. The rate of Lys+ recombinants was derived from the median recombination frequency. The reported values are the mean values with SD indicated in brackets ($n = 3$). (F) Exponentially growing cells were serially diluted (1:10) and spotted out onto YEPD plates with or without HU or MMS. All strains carried *SML1* deletion that kept *mec1Δ* cells viable. (G) Protein extracts prepared from exponentially growing cells were analyzed by western blotting with anti-HA and anti-Myc antibodies either directly (Input) or after immunoprecipitation (IP) with anti-HA antibodies. *indicates a cross-hybridization signal.

2008; Cannavo *et al.* 2018). A region of Sae2 spanning from 120 to 170 amino acids (and therefore containing the S134 residue) was shown to be important for Sae2 self-interaction (Kim *et al.* 2008), prompting us to test the self-association properties of Sae2-ms. Sae2 was immunoprecipitated with anti-HA antibodies from protein extracts of *SAE2-HA/SAE2-MYC*, *sae2-ms-HA/SAE2-MYC* and *sae2-ms-HA/sae2-ms-MYC* diploid cells. The amount of either Sae2-Myc or Sae2-ms-Myc detected by anti-Myc antibodies in immunoprecipitates of Sae2-ms-HA was similar to that of wild-type Sae2-Myc detected in immunoprecipitates of Sae2-HA (Figure 5G). Thus, the *sae2-ms* mutation does not affect Sae2 self-interaction.

Sae2 plays distinct functions in downregulation of MRX-Tel1 and Rad53 activities

Activation of Rad53 requires its interaction with the adaptor Rad9 that is phosphorylated by Mec1/Tel1 (Emili 1998; Sun *et al.* 1998; Vialard *et al.* 1998; Durocher *et al.* 1999; Pellicioli *et al.* 1999; Gilbert *et al.* 2001; Schwartz *et al.* 2002; Sweeney *et al.* 2005; Smolka *et al.* 2007). To better understand the effects of Sae2-ms and Sae2-S134L on Tel1-mediated Rad53 activation, we analyzed Rad9 and Rad53 phosphorylation, detected as electrophoretic mobility shifts, in *mec1*Δ, *sae2*Δ *mec1*Δ, *sae2-ms mec1*Δ, and *sae2-S134L mec1*Δ cells arrested in G1 and then released into the cell cycle in the presence of MMS. As expected, MMS-treated *mec1*Δ cells showed a decrease of both Rad9 (Figure 6A) and Rad53 phosphorylation (Figure 6B) compared to wild type cells. Consistent with the finding that the *sae2*Δ, *sae2-ms*, and *sae2-S134L* alleles increase Tel1 signaling activity, Rad9 phosphorylation was increased in MMS-treated *sae2*Δ *mec1*Δ, *sae2-ms mec1*Δ, and *sae2-S134L mec1*Δ cells compared to *mec1*Δ cells (Figure 6A). However, while *sae2*Δ *mec1*Δ cells showed also enhanced Rad53 phosphorylation compared to *mec1*Δ cells, *sae2-ms mec1*Δ, and *sae2-S134L mec1*Δ cells did not (Figure 6B). The inability of *sae2-ms mec1*Δ and *sae2-S134L mec1*Δ cells to hyperactivate Rad53 compared to *sae2*Δ *mec1*Δ cells is not due to a more efficient DNA repair, as *sae2-ms* and *sae2-S134L* cells did not show Rad53 hyperactivation also in response to a single irreparable DSB (Figure 6C). In fact, when cultures of JKM139 derivative strains were transferred to galactose to induce HO, *sae2*Δ *mec1*Δ cells showed an increased amount of Rad53 phosphorylation compared to *mec1*Δ cells, while neither *sae2-ms mec1*Δ nor *sae2-S134L mec1*Δ cells did (Figure 6C). These findings indicate that Sae2-ms and Sae2-S134L mutant variants are defective in the downregulation of MRX-Tel1 signaling, but not of Rad53 signaling.

Cells carrying a single irreparable DSB undergo checkpoint-mediated cell cycle arrest, but then they adapt to this checkpoint, decreasing Rad53 activation and re-entering the cell cycle (Toczyski *et al.* 1997; Pellicioli *et al.* 2001). The heightened Rad53 activation in *sae2*Δ cells prevents the turning off of the checkpoint triggered by a single irreparable DSB (Clerici *et al.* 2006). To assess further that Tel1/MRX upregulation by Sae2-ms and Sae2-S134L does not increase Rad53 activation, we analyzed the ability of *sae2-ms* and *sae2-S134L* cells to adapt to a single irreparable DSB. When G1-arrested cell cultures of JKM139 derivative strains were spotted on galactose-containing plates to induce HO, most *sae2*Δ cells were still arrested at the two-cell dumbbell stage after 20 hr, whereas wild type, *sae2-ms*, and *sae2-S134L* cells over-rode the checkpoint-mediated cell cycle arrest within 16 hr, producing microcolonies with more than two cells (Figure 6D). Moreover, when galactose was added to exponentially growing cell cultures of the same strains, Rad53 phosphorylation decreased in wild type, *sae2-ms*, and *sae2-S134L* cells 12–14 hr after galactose addition, while it persisted throughout the experiment in *sae2*Δ cells (Figure 6E). Altogether, these findings indicate that Sae2-ms and Sae2-S134L mutant variants are specifically defective in downregulating Tel1 activation but not Rad53 activation, indicating that Sae2 plays distinct functions in the inhibition of MRX-Tel1 and Rad53 activities.

Sae2 inhibits the interaction between Rad9 and Rad53

Activation of Rad53 *in vivo* requires its interaction with Rad9, which acts both as an adaptor mediating the interaction between Mec1 and Rad53, and as a scaffold facilitating the concentration of Rad53 molecules at the sites of damage. In fact, Rad9 phosphorylation by Mec1 or Tel1 creates a binding site for Rad53 interaction (Sun *et al.* 1998; Durocher *et al.* 1999; Schwartz *et al.* 2002). Mec1 and Tel1 subsequently phosphorylate Rad53, which is associated with Rad9 (Sweeney *et al.* 2005; Smolka *et al.* 2007), followed by Rad53 *in trans* autophosphorylation and full activation of the kinase (Pellicioli *et al.* 1999; Gilbert *et al.* 2001).

The finding that Sae2-ms and Sae2-S134L are capable of inducing Rad9 hyperphosphorylation but not Rad53 hyperphosphorylation suggests that Sae2 can inhibit Rad53 activation by limiting Rad53–Rad9 interaction and/or Rad53 autophosphorylation. We therefore immunoprecipitated HA epitope-tagged Rad9 from cell extracts prepared from undamaged exponentially growing cells. A basal level of Rad53 binding to Rad9 was detected in wild-type cells even in the absence of DNA damage, and this interaction increased when Rad9 was immunoprecipitated from *sae2*Δ cells (Figure 7A). By contrast, both *sae2-ms* and *sae2-S134L* cells showed a level of Rad53 binding to Rad9 similar to that observed in wild-type cells (Figure 7A). These findings indicate that Sae2 inhibits Rad53–Rad9 interaction and that Sae2-ms and Sae2-S134L maintain this function. This inhibition does not depend on Sae2 stimulation of MRX nuclease activity, as Rad53 binding to Rad9 in nuclease defective *mre11-H125N* cells was similar to that of wild-type cells or even lower (Figure 7B).

Sae2 overproduction was shown to decrease Rad53 phosphorylation and activation independently of DSB repair (Clerici *et al.* 2006). The ability of Sae2-ms and Sae2-S134L

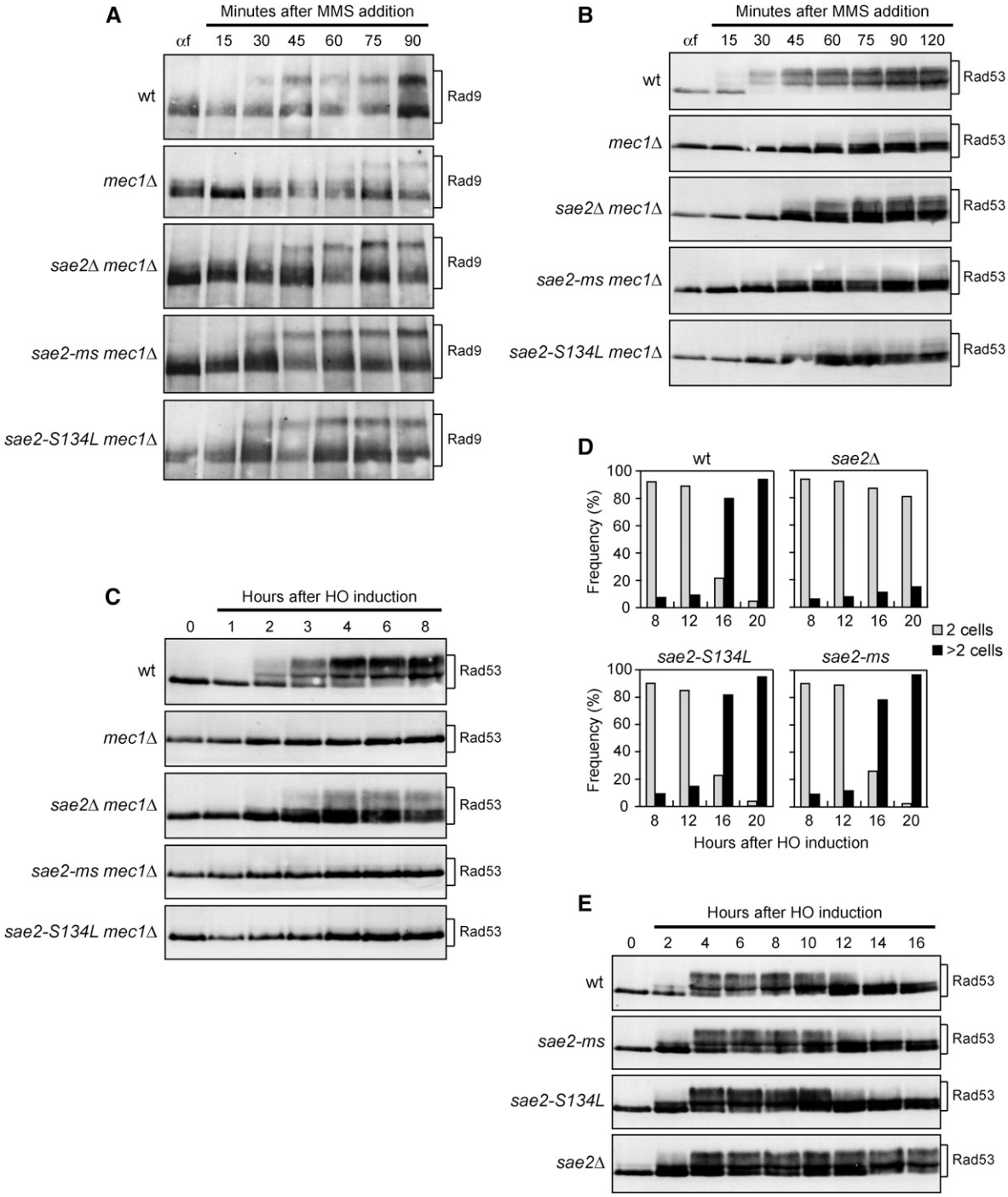

Figure 6 Sae2-ms and Sae2-S134L do not enhance Rad53 phosphorylation. (A and B) Exponentially growing cells were arrested in G1 with α-factor (αf) and released into the cell cycle in the presence of MMS (0.03%). Western blot analysis with anti-Rad9 (A) and anti-Rad53 antibodies (B). (C) Exponentially growing YEPR cultures of JKM139 derivative strains were transferred to YEPRG at time zero to induce HO. Western blot analysis with anti-Rad53 antibodies. (D) Adaptation assay. YEPR G1-arrested cell cultures were plated on galactose-containing plates (time zero). At the indicated time points, 200 cells for each strain were analyzed to determine the frequency of large budded cells (two cells) and of cells forming microcolonies of more than two cells. (E) Exponentially growing YEPR cell cultures were transferred to YEPRG at time zero to induce HO. Western blot analysis with anti-Rad53 antibodies.

to downregulate Rad53 activation is not due to increased production or binding to the sites of damage of the corresponding mutant proteins. In fact, similar amounts of Sae2, Sae2-ms, and Sae2-S134L were detected in protein extracts from wild type, *sae2-ms*, and *sae2-S134L* cells (Figure 7C). Furthermore, the amount of Sae2-ms and Sae2-S134L bound at an HO-induced DSB was similar, or even lower, than that of wild-type Sae2 (Figure 7D).

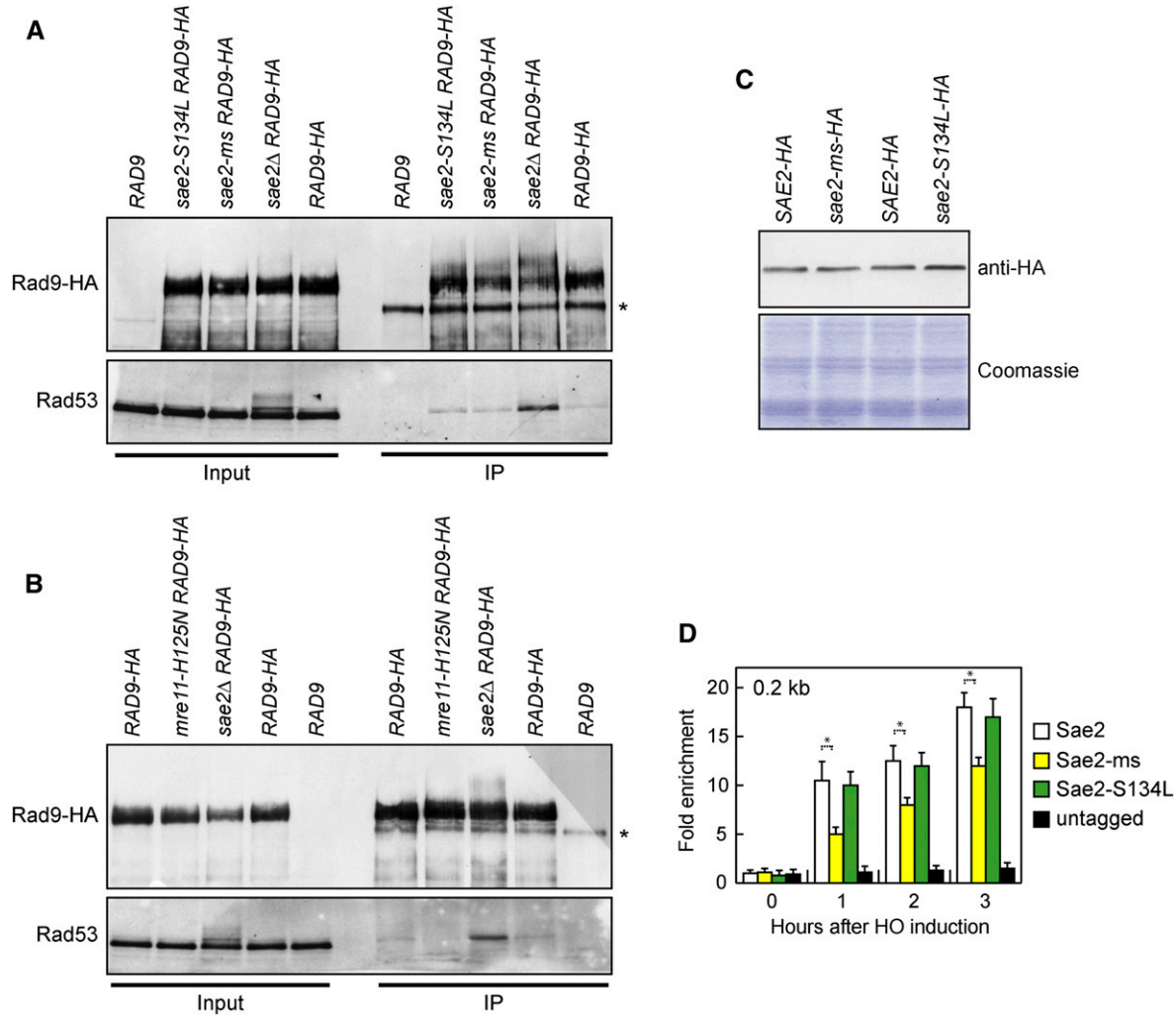

Figure 7 Sae2 inhibits Rad9-Rad53 interaction. (A and B) Protein extracts prepared from exponentially growing cells were analyzed by western blotting with anti-HA (Rad9) and anti-Rad53 antibodies either directly (Input) or after immunoprecipitation (IP) with anti-HA antibodies. *indicates a cross-hybridization signal. (C) Western blot analysis with anti-HA antibodies of protein extracts prepared from exponentially growing cells. The same amount of extracts was stained with Coomassie Blue as loading control. (D) ChIP analysis. HO was induced by galactose addition at time zero in exponentially growing JKM139 derivative cells. Relative fold enrichment of Sae2-HA protein at the indicated distance from the HO cleavage site was determined after ChIP with anti-HA antibodies and subsequent qPCR analysis. Plotted values are the mean values with error bars denoting SD (n = 3). * $P < 0.05$ (Student's t-test).

Discussion

SAE2 deletion causes DNA damage hypersensitivity and enhances Tel1 and Rad53 signaling activities (Usui *et al.* 2001; Lisby *et al.* 2004; Clerici *et al.* 2006). The persistent Tel1- and Rad53-mediated checkpoint activation in *sae2*Δ cells requires the function of MRX, whose association at DSBs is increased in *sae2*Δ cells (Lisby *et al.* 2004; Clerici *et al.* 2006). Reducing either MRX association to DSBs or Rad53/Tel1 signaling restores DNA damage resistance in Sae2-deficient cells (Chen *et al.* 2015; Gobbini *et al.* 2015; Puddu *et al.* 2015; Cassani *et al.* 2018), suggesting that the DNA damage hypersensitivity of *sae2*Δ cells is due to a failure to downregulate MRX/Tel1 and/or Rad53 activities.

To better understand the function of Sae2 in DNA damage resistance and in the regulation of MRX association to DSBs and of Tel1 and Rad53 activation, we searched for *sae2* alleles that hyperactivate Tel1, but that do not cause DNA damage hypersensitivity by themselves. This screen allowed us to identify the Sae2-ms mutant variant, which restores resistance of *mec1*Δ cells to HU and MMS in a Tel1-, Rad9- and Rad53-dependent manner. Sae2-ms carries three amino acid substitutions, with S134L being responsible for *mec1*Δ suppression.

Similar to *SAE2* deletion, both Sae2-ms and Sae2-S134L increase Tel1 signaling activity by enhancing MRX and Tel1 association to DNA ends, and are defective in hairpin cleavage, which is known to depend on Mre11 endonucleolytic activity (Lobachev *et al.* 2002). This finding suggests that the MRX-Sae2-mediated cleavage activity contributes to eliminate MRX bound to DNA ends and this MRX displacement limits Tel1 signaling activity. Consistent with a role of

Mre11 endonuclease in MRX removal, abolition of Mre11 nuclease activity by the H125N substitution increases the amount of MRX and Tel1 bound at DSBs to an extent similar to that caused by *SAE2* deletion.

Upregulation of MRX-Tel1 in *sae2*Δ cells is accompanied by enhanced DSB-induced Rad53 phosphorylation and activation. Although *sae2*Δ, *sae2-ms*, and *sae2-S134L* cells show equivalent increase of MRX and Tel1 association to DSBs, Sae2-ms and Sae2-S134L do not cause persistent Rad53 activation as the absence of Sae2. The inability of *sae2-ms* and *sae2-S134L* cells to hyperactivate Rad53 compared to *sae2*Δ cells does not appear to be due to different amounts of MRX-Tel1 bound to DSBs and/or residual Mre11 clipping activity. In fact, nuclease defective *mre11-H125N* cells, which increase MRX-Tel1 association at DSBs and reduce hairpin cleavage to an extent similar to *sae2*Δ cells, fail to hyperactivate Rad53. These findings suggest that Sae2 plays distinct functions in dampening Tel1 and Rad53 signaling activities.

Mec1 is known to play two distinct roles in Rad53 activation. First, Mec1 phosphorylates multiple Rad9 residues (Schwartz *et al.* 2002), and phosphorylated Rad9 recruits Rad53 to DNA lesions (Sun *et al.* 1998; Vialard *et al.* 1998; Durocher *et al.* 1999; Schwartz *et al.* 2002). Then, Mec1 phosphorylates Rad53 bound to Rad9 on multiple sites (Sweeney *et al.* 2005; Smolka *et al.* 2007), and this phosphorylation of Rad53 presumably contributes to the relief of catalytic autoinhibition, allowing Rad53 autophosphorylation and activation (Pellicioli *et al.* 1999; Gilbert *et al.* 2001). Consistent with an upregulation of Tel1 activity, both the lack of Sae2 and the presence of Sae2-ms or Sae2-S134L increase DSB-induced Rad9 phosphorylation in cells lacking Mec1. However, only the lack of Sae2, but neither the presence Sae2-ms nor Sae2-S134L, increases the interaction between Rad53 and Rad9 even in the absence of DNA lesions. Since Rad53 autophosphorylation and activation requires Mec1/Tel1-dependent phosphorylation of Rad53 molecules that are bound to Rad9 (Sweeney *et al.* 2005), we propose that Sae2 limits Rad53 activation by inhibiting Rad53–Rad9 interaction, and that Sae2-ms and Sae2-S134L maintain this function.

How does Sae2 limit Rad9-Rad53 interaction? Sae2-mediated inhibition of Rad53 activation does not require Sae2 function in promoting MRX nuclease activity, as Rad53–Rad9 interaction is not enhanced in *mre11-H125N* cells. We have previously shown that Rad9 persistence is the primary cause of the DNA damage hypersensitivity and the resection defect of *sae2*Δ cells (Gobbini *et al.* 2015). Interestingly, neither Sae2-ms nor Mre11-H125N increases Rad9 persistence at DSBs. This finding suggests that the Mre11 nuclease activity does not limit Rad9 accumulation at DSBs and that Sae2 by itself can directly interfere with Rad9 persistence at DNA ends. As Rad9 is required to activate Rad53, a robust Rad9 accumulation at DSBs in *sae2*Δ cells can account for the increased Rad9–Rad53 interaction and therefore Rad53 hyperactivation. However, since Sae2 interacts with Rad53 (Liang *et al.* 2015), and defective Rad53 kinase activity bypasses Sae2 function in DNA damage resistance and resection by decreasing the amount of Rad9 bound at DSBs (Gobbini *et al.* 2015), it is also possible that Sae2 directly inhibits Rad9–Rad53 interaction, and that the lack of this function leads to Rad53 hyperactivation, which in turn increases Rad9 association to DSBs in a positive feedback loop. In any case, the finding that *sae2-ms* and *sae2-S134L* are proficient in long-range resection, and are DNA damage resistant, indicates that the increased Rad9 accumulation at DSBs is responsible for the DNA damage hypersensitivity and the impaired long-range resection of *sae2*Δ cells.

Although Rad53 is not hyperactivated in both *sae2-ms* and *sae2-S134L* cells as in *sae2*Δ cells, both Sae2-ms and Sae2-S134L are capable of compensating for Mec1 deficiency in a Rad53-dependent manner. This finding suggests that upregulation of MRX/Tel1 signaling by these Sae2 mutant variants increases Rad53 activation to a level that is sufficient to compensate for Mec1 deficiency. However, as Rad9 persistence at DSBs is not enhanced in these cells compared to *sae2*Δ cells, the retained ability of Sae2-ms and Sae2-S134L to limit Rad9 accumulation at DSBs does not allow to reach the extent of Rad53 activation that is responsible for the persistent DNA damage-induced cell cycle arrest of *sae2*Δ cells.

Although the nuclease defective Mre11-H125N variant increases MRX and Tel1 accumulation at DSBs, unlike Sae2-ms and Sae2-S134L, it is not capable to compensate for Mec1 deficiency. Interestingly, the Mre11-H125N mutant variant was shown to increase the amount of Sae2 bound at DSBs (Lisby *et al.* 2004). As Sae2 overproduction decreases Rad53 phosphorylation and activation (Clerici *et al.* 2006), the increased Sae2 persistence at DSBs in *mre11-H125N* cells may limit Rad53 activation, and, therefore, the ability of Mre11-H125N to compensate for Mec1 deficiency despite an increased MRX-Tel1 signaling. As Rad9 and Rad53 limit DSB resection by inhibiting Sgs1/Dna2 and Exo1 (Morin *et al.* 2008; Bonetti *et al.* 2015; Ferrari *et al.* 2015; Gobbini *et al.* 2015), downregulation of both Rad9 persistence at DSBs and Rad53 activation can also explain why *mre11-H125N* cells are proficient in long-range resection and are considerably less sensitive to DNA damaging agents than *sae2*Δ cells.

In summary, our findings support a model whereby Sae2 has two distinct functions in checkpoint downregulation. On the one hand, it removes MRX and Tel1 from DNA ends by promoting Mre11 endonuclease activity; on the other, it limits Rad9 accumulation to DSBs independently of Mre11 nuclease activity. Both these Sae2 functions contribute to downregulate Rad53 activation, with control of Rad9 association playing the major role, providing different layers of regulation of the checkpoint response in the maintenance of genome stability.

Acknowledgments

We thank G. Lucchini for critical reading of the manuscript. We also thank J. Haber, M. A. Resnick, and D.P. Toczyski for yeast strains, and J. Diffley and N. Lowndes for antibodies.

The research leading to these results has received funding from Associazione Italiana per la Ricerca sul Cancro (AIRC) under IG 2017 – ID. 19783 project – P.I. Longhese Maria Pia, and Progetti di Ricerca di Interesse Nazionale (PRIN) 2015 to M.P.L.

Literature Cited

Berkovich, E., R. J. Jr. Monnat, and M. B. Kastan, 2007 Roles of ATM and NBS1 in chromatin structure modulation and DNA double-strand break repair. Nat. Cell Biol. 9: 683–690. https://doi.org/10.1038/ncb1599

Bonetti, D., M. Villa, E. Gobbini, C. Cassani, G. Tedeschi *et al.*, 2015 Escape of Sgs1 from Rad9 inhibition reduces the requirement for Sae2 and functional MRX in DNA end resection. EMBO Rep. 16: 351–361. https://doi.org/10.15252/embr.201439764

Bonetti, D., C. V. Colombo, M. Clerici, and M. P. Longhese, 2018 Processing of DNA ends in the maintenance of genome stability. Front. Genet. 9: 390. https://doi.org/10.3389/fgene.2018.00390

Cannavo, E., and P. Cejka, 2014 Sae2 promotes dsDNA endonuclease activity within Mre11-Rad50-Xrs2 to resect DNA breaks. Nature 514: 122–125. https://doi.org/10.1038/nature13771

Cannavo, E., P. Cejka, and S. C. Kowalczykowski, 2013 Relationship of DNA degradation by *Saccharomyces cerevisiae* exonuclease 1 and its stimulation by RPA and Mre11-Rad50-Xrs2 to DNA end resection. Proc. Natl. Acad. Sci. USA 110: E1661–E1668. https://doi.org/10.1073/pnas.1305166110

Cannavo, E., D. Johnson, S. N. Andres, V. M. Kissling, J. K. Reinert *et al.*, 2018 Regulatory control of DNA end resection by Sae2 phosphorylation. Nat. Commun. 9: 4016. https://doi.org/10.1038/s41467-018-06417-5

Cassani, C., E. Gobbini, W. Wang, H. Niu, M. Clerici *et al.*, 2016 Tel1 and Rif2 regulate MRX function in end-tethering and repair of DNA double-strand breaks. PLoS Biol. 14: e1002387. https://doi.org/10.1371/journal.pbio.1002387

Cassani, C., E. Gobbini, J. Vertemara, W. Wang, A. Marsella *et al.*, 2018 Structurally distinct Mre11 domains mediate MRX functions in resection, end-tethering and DNA damage resistance. Nucleic Acids Res. 46: 2990–3008. https://doi.org/10.1093/nar/gky086

Cejka, P., E. Cannavo, P. Polaczek, T. Masuda-Sasa, S. Pokharel *et al.*, 2010 DNA end resection by Dna2-Sgs1-RPA and its stimulation by Top3-Rmi1 and Mre11-Rad50-Xrs2. Nature 467: 112–116. https://doi.org/10.1038/nature09355

Chen, H., R. A. Donnianni, N. Handa, S. K. Deng, J. Oh *et al.*, 2015 Sae2 promotes DNA damage resistance by removing the Mre11-Rad50-Xrs2 complex from DNA and attenuating Rad53 signaling. Proc. Natl. Acad. Sci. USA 112: E1880–E1887. https://doi.org/10.1073/pnas.1503331112

Ciccia, A., and S. J. Elledge, 2010 The DNA damage response: making it safe to play with knives. Mol. Cell 40: 179–204. https://doi.org/10.1016/j.molcel.2010.09.019

Clerici, M., D. Mantiero, G. Lucchini, and M. P. Longhese, 2005 The *Saccharomyces cerevisiae* Sae2 protein promotes resection and bridging of double strand break ends. J. Biol. Chem. 280: 38631–38638. https://doi.org/10.1074/jbc.M508339200

Clerici, M., D. Mantiero, G. Lucchini, and M. P. Longhese, 2006 The *Saccharomyces cerevisiae* Sae2 protein negatively regulates DNA damage checkpoint signalling. EMBO Rep. 7: 212–218. https://doi.org/10.1038/sj.embor.7400593

Clerici, M., C. Trovesi, A. Galbiati, G. Lucchini, and M. P. Longhese, 2014 Mec1/ATR regulates the generation of single-stranded DNA that attenuates Tel1/ATM signaling at DNA ends. EMBO J. 33: 198–216. https://doi.org/10.1002/embj.201386041

Colombo, C. V., L. Menin, and M. Clerici, 2018 Alkaline denaturing southern blot analysis to monitor double-strand break processing. Methods Mol. Biol. 1672: 131–145. https://doi.org/10.1007/978-1-4939-7306-4_11

Debrauwère, H., S. Loeillet, W. Lin, J. Lopes, and A. Nicolas, 2001 Links between replication and recombination in *Saccharomyces cerevisiae*: a hypersensitive requirement for homologous recombination in the absence of Rad27 activity. Proc. Natl. Acad. Sci. USA 98: 8263–8269. https://doi.org/10.1073/pnas.121075598

Durocher, D., J. Henckel, A. R. Fersht, and S. P. Jackson, 1999 The FHA domain is a modular phosphopeptide recognition motif. Mol. Cell 4: 387–394. https://doi.org/10.1016/S1097-2765(00)80340-8

Emili, A., 1998 *MEC1*-dependent phosphorylation of Rad9p in response to DNA damage. Mol. Cell 2: 183–189. https://doi.org/10.1016/S1097-2765(00)80128-8

Falck, J., J. Coates, and S. P. Jackson, 2005 Conserved modes of recruitment of ATM, ATR and DNA-PKcs to sites of DNA damage. Nature 434: 605–611. https://doi.org/10.1038/nature03442

Ferrari, M., D. Dibitetto, G. De Gregorio, V. V. Eapen, C. C. Rawal *et al.*, 2015 Functional interplay between the 53BP1-ortholog Rad9 and the Mre11 complex regulates resection, end-tethering and repair of a double-strand break. PLoS Genet. 11: e1004928. https://doi.org/10.1371/journal.pgen.1004928

Fishman-Lobell, J., N. Rudin, and J. E. Haber, 1992 Two alternative pathways of double-strand break repair that are kinetically separable and independently modulated. Mol. Cell. Biol. 12: 1292–1303. https://doi.org/10.1128/MCB.12.3.1292

Fu, Q., J. Chow, K. A. Bernstein, N. Makharashvili, S. Arora *et al.*, 2014 Phosphorylation-regulated transitions in an oligomeric state control the activity of the Sae2 DNA repair enzyme. Mol. Cell. Biol. 34: 778–793 (erratum: Mol. Cell Biol. 34: 4213). https://doi.org/10.1128/MCB.00963-13

Garcia, V., S. E. Phelps, S. Gray, and M. J. Neale, 2011 Bidirectional resection of DNA double-strand breaks by Mre11 and Exo1. Nature 479: 241–244. https://doi.org/10.1038/nature10515

Gilbert, C. S., C. M. Green, and N. F. Lowndes, 2001 Budding yeast Rad9 is an ATP-dependent Rad53 activating machine. Mol. Cell 8: 129–136. https://doi.org/10.1016/S1097-2765(01)00267-2

Gobbini, E., D. Cesena, A. Galbiati, A. Lockhart, and M. P. Longhese, 2013 Interplays between ATM/Tel1 and ATR/Mec1 in sensing and signaling DNA double-strand breaks. DNA Repair (Amst.) 12: 791–799. https://doi.org/10.1016/j.dnarep.2013.07.009

Gobbini, E., M. Villa, M. Gnugnoli, L. Menin, M. Clerici *et al.*, 2015 Sae2 function at DNA double-strand breaks is bypassed by dampening Tel1 or Rad53 activity. PLoS Genet. 11: e1005685. https://doi.org/10.1371/journal.pgen.1005685

Gobbini, E., C. Cassani, J. Vertemara, W. Wang, F. Mambretti *et al.*, 2018 The MRX complex regulates Exo1 resection activity by altering DNA end structure. EMBO J. 337: e98701. https://doi.org/10.15252/embj.201798588

Hardy, J., D. Churikov, V. Géli, and M. N. Simon, 2014 Sgs1 and Sae2 promote telomere replication by limiting accumulation of ssDNA. Nat. Commun. 5: 5004. https://doi.org/10.1038/ncomms6004

Huertas, P., F. Cortés-Ledesma, A. A. Sartori, A. Aguilera, and S. P. Jackson, 2008 CDK targets Sae2 to control DNA-end resection and homologous recombination. Nature 455: 689–692. https://doi.org/10.1038/nature07215

Ivanov, E. L., N. Sugawara, J. Fishman-Lobell, and J. E. Haber, 1996 Genetic requirements for the single-strand annealing pathway of double-strand break repair in *Saccharomyces cerevisiae*. Genetics 142: 693–704.

Jazayeri, A., J. Falck, C. Lukas, J. Bartek, G. C. Smith *et al.*, 2006 ATM- and cell cycle-dependent regulation of ATR in response to DNA double-strand breaks. Nat. Cell Biol. 8: 37–45. https://doi.org/10.1038/ncb1337

Kim, H. S., S. Vijayakumar, M. Reger, J. C. Harrison, J. E. Haber *et al.*, 2008 Functional interactions between Sae2 and the Mre11 complex. Genetics 178: 711–723. https://doi.org/10.1534/genetics.107.081331

Lee, J. H., and T. T. Paull, 2005 ATM activation by DNA double-strand breaks through the Mre11-Rad50-Nbs1 complex. Science 308: 551–554. https://doi.org/10.1126/science.1108297

Lee, S. E., J. K. Moore, A. Holmes, K. Umezu, R. D. Kolodner *et al.*, 1998 *Saccharomyces* Ku70, Mre11/Rad50 and RPA proteins regulate adaptation to G2/M arrest after DNA damage. Cell 94: 399–409. https://doi.org/10.1016/S0092-8674(00)81482-8

Liang, J., R. T. Suhandynata, and H. Zhou, 2015 Phosphorylation of Sae2 mediates forkhead-associated (FHA) domain-specific interaction and regulates its DNA repair function. J. Biol. Chem. 290: 10751–10763. https://doi.org/10.1074/jbc.M114.625293

Lisby, M., J. H. Barlow, R. C. Burgess, and R. Rothstein, 2004 Choreography of the DNA damage response: spatiotemporal relationships among checkpoint and repair proteins. Cell 118: 699–713. https://doi.org/10.1016/j.cell.2004.08.015

Llorente, B., and L. S. Symington, 2004 The Mre11 nuclease is not required for 5′ to 3′ resection at multiple HO-induced double-strand breaks. Mol. Cell. Biol. 24: 9682–9694. https://doi.org/10.1128/MCB.24.21.9682-9694.2004

Lobachev, K. S., D. A. Gordenin, and M. A. Resnick, 2002 The Mre11 complex is required for repair of hairpin-capped double-strand breaks and prevention of chromosome rearrangements. Cell 108: 183–193. https://doi.org/10.1016/S0092-8674(02)00614-1

Mehta, A., and J. E. Haber, 2014 Sources of DNA double-strand breaks and models of recombinational DNA repair. Cold Spring Harb. Perspect. Biol. 6: a016428. https://doi.org/10.1101/cshperspect.a016428

Mimitou, E. P., and L. S. Symington, 2008 Sae2, Exo1 and Sgs1 collaborate in DNA double-strand break processing. Nature 455: 770–774. https://doi.org/10.1038/nature07312

Moreau, S., J. R. Ferguson, and L. S. Symington, 1999 The nuclease activity of Mre11 is required for meiosis but not for mating type switching, end joining, or telomere maintenance. Mol. Cell. Biol. 19: 556–566. https://doi.org/10.1128/MCB.19.1.556

Morin, I., H. P. Ngo, A. Greenall, M. K. Zubko, N. Morrice *et al.*, 2008 Checkpoint-dependent phosphorylation of Exo1 modulates the DNA damage response. EMBO J. 27: 2400–2410. https://doi.org/10.1038/emboj.2008.171

Myers, J. S., and D. Cortez, 2006 Rapid activation of ATR by ionizing radiation requires ATM and Mre11. J. Biol. Chem. 281: 9346–9350. https://doi.org/10.1074/jbc.M513265200

Nakada, D., K. Matsumoto, and K. Sugimoto, 2003 ATM-related Tel1 associates with double-strand breaks through an Xrs2-dependent mechanism. Genes Dev. 17: 1957–1962. https://doi.org/10.1101/gad.1099003

Neale, M. J., J. Pan, and S. Keeney, 2005 Endonucleolytic processing of covalent protein-linked DNA double-strand breaks. Nature 436: 1053–1057. https://doi.org/10.1038/nature03872

Nicolette, M. L., K. Lee, Z. Guo, M. Rani, J. M. Chow *et al.*, 2010 Mre11-Rad50-Xrs2 and Sae2 promote 5′ strand resection of DNA double-strand breaks. Nat. Struct. Mol. Biol. 17: 1478–1485. https://doi.org/10.1038/nsmb.1957

Nimonkar, A. V., J. Genschel, E. Kinoshita, P. Polaczek, J. L. Campbell *et al.*, 2011 BLM-DNA2-RPA-MRN and EXO1-BLM-RPA-MRN constitute two DNA end resection machineries for human DNA break repair. Genes Dev. 25: 350–362. https://doi.org/10.1101/gad.2003811

Niu, H., W. H. Chung, Z. Zhu, Y. Kwon, W. Zhao *et al.*, 2010 Mechanism of the ATP-dependent DNA end-resection machinery from *Saccharomyces cerevisiae*. Nature 467: 108–111. https://doi.org/10.1038/nature09318

Pellicioli, A., C. Lucca, G. Liberi, F. Marini, M. Lopes *et al.*, 1999 Activation of Rad53 kinase in response to DNA damage and its effect in modulating phosphorylation of the lagging strand DNA polymerase. EMBO J. 18: 6561–6572. https://doi.org/10.1093/emboj/18.22.6561

Pellicioli, A., S. E. Lee, C. Lucca, M. Foiani, and J. E. Haber, 2001 Regulation of *Saccharomyces* Rad53 checkpoint kinase during adaptation from DNA damage-induced G2/M arrest. Mol. Cell 7: 293–300. https://doi.org/10.1016/S1097-2765(01)00177-0

Puddu, F., T. Oelschlaegel, I. Guerini, N. J. Geisler, H. Niu *et al.*, 2015 Synthetic viability genomic screening defines Sae2 function in DNA repair. EMBO J. 34: 1509–1522. https://doi.org/10.15252/embj.201590973

Reginato, G., E. Cannavo, and P. Cejka, 2017 Physiological protein blocks direct the Mre11-Rad50-Xrs2 and Sae2 nuclease complex to initiate DNA end resection. Genes Dev. 31: 2325–2330. https://doi.org/10.1101/gad.308254.117

Ritchie, K. B., J. C. Mallory, and T. D. Petes, 1999 Interactions of *TLC1* (which encodes the RNA subunit of telomerase), *TEL1*, and *MEC1* in regulating telomere length in the yeast *Saccharomyces cerevisiae*. Mol. Cell. Biol. 19: 6065–6075. https://doi.org/10.1128/MCB.19.9.6065

Schwartz, M. F., J. K. Duong, Z. Sun, J. S. Morrow, D. Pradhan *et al.*, 2002 Rad9 phosphorylation sites couple Rad53 to the *Saccharomyces cerevisiae* DNA damage checkpoint. Mol. Cell 9: 1055–1065. https://doi.org/10.1016/S1097-2765(02)00532-4

Shibata, A., D. Moiani, A. S. Arvai, J. Perry, S. M. Harding *et al.*, 2014 DNA double-strand break repair pathway choice is directed by distinct MRE11 nuclease activities. Mol. Cell 53: 7–18 (erratum: Mol. Cell 53: 361). https://doi.org/10.1016/j.molcel.2013.11.003

Shim, E. Y., W. H. Chung, M. L. Nicolette, Y. Zhang, M. Davis *et al.*, 2010 *Saccharomyces cerevisiae* Mre11/Rad50/Xrs2 and Ku proteins regulate association of Exo1 and Dna2 with DNA breaks. EMBO J. 29: 3370–3380. https://doi.org/10.1038/emboj.2010.219

Smolka, M. B., C. P. Albuquerque, S. H. Chen, and H. Zhou, 2007 Proteome-wide identification of in vivo targets of DNA damage checkpoint kinases. Proc. Natl. Acad. Sci. USA 104: 10364–10369. https://doi.org/10.1073/pnas.0701622104

Sun, Z., J. Hsiao, D. S. Fay, and D. F. Stern, 1998 Rad53 FHA domain associated with phosphorylated Rad9 in the DNA damage checkpoint. Science 281: 272–274. https://doi.org/10.1126/science.281.5374.272

Sweeney, F. D., F. Yang, A. Chi, J. Shabanowitz, D. F. Hunt *et al.*, 2005 *Saccharomyces cerevisiae* Rad9 acts as a Mec1 adaptor to allow Rad53 activation. Curr. Biol. 15: 1364–1375. https://doi.org/10.1016/j.cub.2005.06.063

Tishkoff, D. X., N. Filosi, G. M. Gaida, and R. D. Kolodner, 1997 A novel mutation avoidance mechanism dependent on *S. cerevisiae RAD27* is distinct from DNA mismatch repair. Cell 88: 253–263. https://doi.org/10.1016/S0092-8674(00)81846-2

Toczyski, D. P., D. J. Galgoczy, and L. H. Hartwell, 1997 CDC5 and CKII control adaptation to the yeast DNA damage checkpoint. Cell 90: 1097–1106. https://doi.org/10.1016/S0092-8674(00)80375-X

Trovesi, C., M. Falcettoni, G. Lucchini, M. Clerici, and M. P. Longhese, 2011 Distinct Cdk1 requirements during single-strand annealing, crossover, and noncrossover recombination. PLoS Genet. 7: e1002263. https://doi.org/10.1371/journal.pgen.1002263

Trujillo, K. M., and P. Sung, 2001 DNA structure-specific nuclease activities in the *Saccharomyces cerevisiae* Rad50*Mre11 complex. J. Biol. Chem. 276: 35458–35464. https://doi.org/10.1074/jbc.M105482200

Usui, T., H. Ogawa, and J. H. Petrini, 2001 A DNA damage response pathway controlled by Tel1 and the Mre11 complex. Mol. Cell 7: 1255–1266. https://doi.org/10.1016/S1097-2765(01)00270-2

Vaze, M. B., A. Pellicioli, S. E. Lee, G. Ira, G. Liberi *et al.*, 2002 Recovery from checkpoint-mediated arrest after repair of a double-strand break requires Srs2 helicase. Mol. Cell 10: 373–385. https://doi.org/10.1016/S1097-2765(02)00593-2

Vialard, J. E., C. S. Gilbert, C. M. Green, and N. F. Lowndes, 1998 The budding yeast Rad9 checkpoint protein is subjected to Mec1/Tel1-dependent hyperphosphorylation and interacts with Rad53 after DNA damage. EMBO J. 17: 5679–5688. https://doi.org/10.1093/emboj/17.19.5679

Villa, M., C. Cassani, E. Gobbini, D. Bonetti, and M. P. Longhese, 2016 Coupling end resection with the checkpoint response at DNA double-strand breaks. Cell. Mol. Life Sci. 73: 3655–3663. https://doi.org/10.1007/s00018-016-2262-6

Wang, W., J. M. Daley, Y. Kwon, D. S. Krasner, and P. Sung, 2017 Plasticity of the Mre11-Rad50-Xrs2-Sae2 nuclease ensemble in the processing of DNA-bound obstacles. Genes Dev. 31: 2331–2336. https://doi.org/10.1101/gad.307900.117

You, Z., C. Chahwan, J. Bailis, T. Hunter, and P. Russell, 2005 ATM activation and its recruitment to damaged DNA require binding to the C terminus of Nbs1. Mol. Cell. Biol. 25: 5363–5379. https://doi.org/10.1128/MCB.25.13.5363-5379.2005

Zhu, Z., W. H. Chung, E. Y. Shim, S. E. Lee, and G. Ira, 2008 Sgs1 helicase and two nucleases Dna2 and Exo1 resect DNA double-strand break ends. Cell 134: 981–994. https://doi.org/10.1016/j.cell.2008.08.037

Zou, L., and S. J. Elledge, 2003 Sensing DNA damage through ATRIP recognition of RPA-ssDNA complexes. Science 300: 1542–1548. https://doi.org/10.1126/science.1083430

Communicating editor: O. Cohen-Fix